

## targeted traveling wave MRI

M. Mueller<sup>1</sup>, S. Alt<sup>2</sup>, R. Umathum<sup>2</sup>, W. Semmler<sup>2</sup>, and M. Bock<sup>2</sup>

<sup>1</sup>DKFZ, Heidelberg, Baden-Württemberg, Germany, <sup>2</sup>DKFZ

### Introduction

At high magnetic field strengths, travelling wave MRI can be used to solve the standing wave problem of volume resonators [1]. However, travelling wave MRI suffers from electromagnetic field-attenuation and high whole body energy deposition (SAR), so that only the distal parts of the body can be imaged.

In this work we introduce a new travelling wave RF coil. The coil guides the travelling wave to any desired region in the body and thus limits the whole-body SAR. For wave guidance, a coaxial RF structure is designed, which utilizes a central gap to illuminate the target region.

### Materials and Methods

The coil is based on a coaxial wave guide with an outer- and inner conductor which guides RF travelling waves at a defined TEM mode given by the geometry of the two conductors around the patient (Fig. 1a). A prototype coil was built using a poly-methylmethacrylat (PMMA) tube as coil former (Fig. 1b). To couple the RF field into the imaging object (patient) at the center of the coil, the inner conductor was divided into two parts. The length of the central imaging gap can be varied from 0 mm up to 550 mm. The coil is a down-scaled model of a human-size coil at a ratio of 1:2. The inner-(diameter: 250mm) and outer-(diameter: 300mm) conductors are connected to a matching network (for source- and energy dump connection) by a flexible copper ring with six feed points on both tube ends. A special conductor arrangement was designed on the formers to avoid gradient-induced eddy-currents. Therefore, strips of copper (length: 168mm width: 50mm, thickness: 38 $\mu$ m) were overlapped to achieve capacitive coupling (s. Fig. 2). Between the two copper layers a dielectric polyethylene layer (thickness: 18 $\mu$ m) was placed (Fig. 2). The layer inhibits low-frequency eddy currents, but facilitates the transmission of the traveling RF-waves at the resonance frequency of the 7T MR system (Magnetom 7T, Siemens, Erlangen, Germany,  $f_{res} = 300$  MHz). The strips also overlap in angular orientation to make the inner conductor RF-impermeable. For the imaging experiments a cylindrical PMMA phantom was placed symmetrically in the coil. The cylinder contained H<sub>2</sub>O with isotonic saline solution (0.9% NaCl). The space between the phantom and to the inner conductors was covered with two segmented copper-cloth shielding-caps. The caps were integrated to focus the RF into the imaging gap and to minimize SAR in non imaging areas. The coil was connected to the 7 Tesla MR system, and a relative flip angle map was measured using a FLASH pulse sequence with different nominal flip angles (2D FLASH, TR = 1000 ms, TE = 5.8 ms, matrix size = 64 $\times$ 64; spatial resolution = 4 mm). Images were acquired at 28 different nominal flip angles between 4 $^\circ$  and 112 $^\circ$ . To assess the relative  $B_1$  map, the flip angle at maximum signal (Ernst angle) was determined from the image series by a non-linear least squares fit. To demonstrate the functional capability of the coaxial system a salmon trout (length: 480mm; height: 120mm) was imaged (3D FLASH, nonselective excitation, TR = 12 ms, TE=5.0 ms, matrix size = 128 $\times$ 512; spatial resolution = 1mm).

### Results and Discussion

In the prototype coil following reflection parameters were measured:  $S_{11} = -37$  dB,  $S_{22} = -40$  dB;  $S_{12} = S_{21} = -7.7$ dB. Fig. 3 shows an image of the phantom and the corresponding  $B_1$ -map in transverse orientation. The  $B_1$  field has a minimum at the center and increases towards the phantom edge. In between a radius of 25 mm and 70 mm the maximum field deviation in units of the average is 7.5%, and the mean square deviation is 4.4%. Figure 4 shows the central slices (left) of the phantom in coronal orientation and one slice 20 mm above the center (right). The red lines mark the position of the RF-shielding caps. As intended the  $B_1$  field is mainly located between the RF-shielding caps. At off-center positions a homogenous  $B_1$  field distribution is achieved. Figure 5 shows the 7T image of a 480mm long salmon trout (medial coronal slice). As desired only the anatomy in the imaging gap of 250mm is imaged. Beyond the gap the signal decays fast suggesting marginal SAR in this region. This work presents a technique, which on the one hand solves the standing wave problematic, but keeps the SAR low, because of the showed field-decay beyond the imaging gap and it allows to image any region of the imaging object. To optimize the homogeneity in radial direction we aim to shift the position of the  $B_1$ -field-minimum by an unsymmetrical amplitude excitation at the feed points. Future work is needed for optimization, e.g. to combine the coil concept with local receive coil arrays.

### References

- [1] Brunner et al, Nature 2009 457(7232)
- [2] SEMCAD x v14, Speag, Zürich, Switzerland
- [3] [http://www.itis.ethz.ch/index/index\\_humanmodels.html](http://www.itis.ethz.ch/index/index_humanmodels.html)

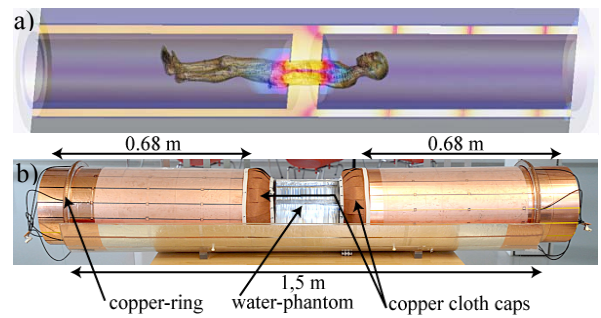


Fig. 1: coaxial wave-guide. a) CAD-simulation-model [2] with a “virtual family” [3] member. Inner conductor gap: 250mm. b) prototype coil with half-open outer conductor (bottom), inner conductor with 200mm gap and a 1.5m\*0.18m water phantom inside

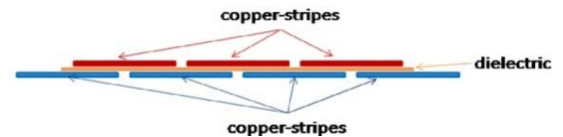


Fig. 2: capacitive array of the inner and outer conductor with two overlaid copper stripe layers and a dielectric sheet (side view)

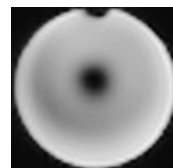


Fig. 3: transversal slice of the 18 litre phantom (left) and a  $B_1$ -map (right)

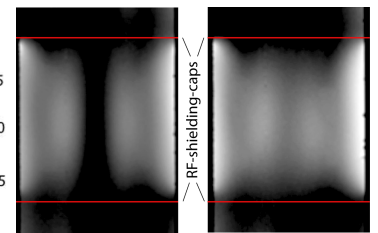


Fig. 4: coronal slice of the phantom center (left) and 20mm above the center (right)

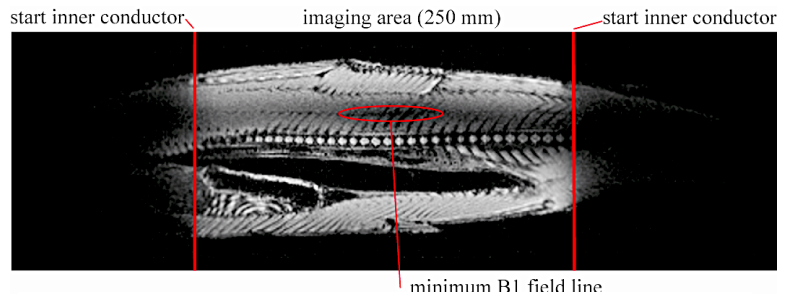


Fig. 5: Salmon trout (480mm length) imaging; medial coronal slice. SAR-limitation by segmented HF-shielding-caps on the left and right (red line).